Award: DE-SC00159274

Recipient: Central Michigan University

PI: Matthew Redshaw

Project Title: High Precision Penning Trap Measurements of β-decay Q-values for Neutrino Physics

Final Progress Report, Due April 30th 2022

Executive Summary

The 2015 Nobel Prize in physics was awarded to Takaaki Kajita and Arthur B McDonald *"for the discovery of neutrino oscillations, which shows that neutrinos have mass"*. This fact has wide reaching implications for the standard model of particle physics, nuclear physics, and cosmology. However, important fundamental questions remain: *What is the absolute neutrino mass scale? Is the neutrino a Majorana or a Dirac particle?* A number of large-scale experiments are underway or are being developed to attempt to answer these questions. Two classes of experiments are direct neutrino mass determination experiments, and searches for neutrinoless double beta-decay.

This work aimed to aid these experiments via high-precision Q value determinations for the relevant isotopes using Penning trap mass spectrometry (PTMS). One of the main objectives for this proposal was to use PTMS to search for isotopes that could have an ultra-low Q-value beta-decay branch (Q < 1 keV). Such a decay would occur between the ground state of the parent isotope and an excited nuclear state in the daughter. In many cases it is unclear as to whether an ultra-low Q-value decay is energetically allowed because of the uncertainty in the atomic masses of the parent and daughter atoms. A second major objective of this work was to construct an ultra-high precision Penning trap to determine the Q-values of Re-187 and Ho-163 to ~1 eV, which is necessary for planned neutrino mass determination experiments with these isotopes. Additional objectives were to measure double beta-decay and double electron capture (2EC) Q-values for evaluating possible future neutrinoless double beta-decay experiments, and to investigate other rare decay processes, such as highly forbidden beta-decays, that could have an impact on neutrino and nuclear physics and on highly sensitive decay experiments.

This project has resulted in a series of precise Q value measurements using facilities at the National Superconducting Cyclotron Facility/Facility for Rare Isotope Beams and Argonne National Laboratory. Potential ultra-low Q value decay branches in Sr-89, Ba-139, Ag-112,113, and Cd-115 have been investigated, and an evaluation of beta-decays across the chart of nuclei has been performed to search for other potential ultra-low Q value beta-decays. Precise Q values for forbidden decays of the long-lived isotopes La-138 and Lu-176 have been performed and used in the analysis of precise beta-spectrum measurements and calculations with these isotopes. The CHIP-TRAP facility has been designed, fabricated and constructed, and initial commissioning of the ion traps has been successfully completed. A laser ablation ion source and a novel Penning ion trap source were developed and commissioned, and a compact multi-reflection time of flight mass separator was designed and is being commissioned to enable high sensitivity to isotopes that are only available in small quantities, such as long-lived radioactive isotopes.

Goals, Objectives and Actual Accomplishments of the Project

The main objective of this project was to use Penning trap mass spectrometry (PTMS) to perform high-precision Q value measurements for isotopes relevant to experiments that aim to determine properties of the neutrino, such as the absolute mass scale and the neutrino's Dirac or Majorana particle nature. There were three main goals in the research that our group undertook in order to fulfill this objective:

A) Design and construction of CHIP-TRAP

Goal: Construct an ultra-high precision Penning trap mass spectrometer – the CMU high-precision Penning trap (CHIP-TRAP) – to be used to determine the Q values of ^{187}Re and ^{163}Ho to ~1 eV for direct neutrino mass determination experiments.

Accomplishments:

- Fabrication and installation of Penning traps.
- Design, fabrication, assembly, installation and commissioning of beam line.
- Commissioning of laser ablation ion source (LAS).
  Published in Hyperfine Interactions: https://doi.org/10.1007/s10751-019-1617-4
- Conceptualization, design, fabrication, and commissioning of a Penning ion trap source.
- Design, fabrication, installation and commissioning of a multi-reflection time of flight mass separator (MR-TOF-MS).

B) Ultra-low Q value β-decay measurements

Goal: Search for isotopes with an energetically allowed β-decay branch to an excited state in the daughter nuclide with an ultra-low Q value (<1 keV) determined using PTMS.

Accomplishments:

- Measurement at CPT of ^{112,113}Ag, and ^{115}Cd β-decay Q values
  Submitted to PRC: https://arxiv.org/abs/2202.12874
- Measurement at NSCL of ^{89}Y, ^{138}La masses to evaluate ^{89}Sr, ^{138}Ba β-decay Q values.
  Published in PRC: https://doi.org/10.1103/PhysRevC.100.024309
- Measurement of mass of ^{75}As at NSCL to evaluate UL Q value branches in ^{75}Se and ^{75}Ge (analysis in progress).
- Evaluation of all potential UL Q value β-decay candidates
  Published in Hyperfine Interactions: https://doi.org/10.1007/s10751-019-1588-5
  2022 update submitted to PRC: https://arxiv.org/abs/2201.08790

C) β-decay and double β-decay Q value measurements

Goal: Perform precise measurements of ββ-decay and 2EC Q values using PTMS for evaluating searches for neutrinoless ββ-decay, and measurements of other β-decay Q values, such as highly forbidden β-decays that could impact neutrino physics experiments.

Accomplishments:

- Measurement of ^{50}V 4th forbidden β-decay and electron capture Q values
  Published in PRC: https://doi.org/10.1103/PhysRevC.96.044321
- Measurement of the ^{138}La 2nd forbidden β-decay Q value.
  Published in PRC: https://doi.org/10.1103/PhysRevC.100.014308
- Measurement of the ^{176}Lu 1st forbidden β-decay Q value (in preparation).
- Proposal for a measurement of the ^{48}Sc – ^{48}Ca 5th forbidden β-decay Q value at TRIUMF (experiment approved).
- Measurement of the ^{7}Be electron capture Q value at NSCL (analysis in progress).

Summary of Project Activity

A) Design and construction of CHIP-TRAP

Year 1 (Jul 2016 – Jun 2017):

During this first year of the project, we began the initial design phase of the CMU high-precision Penning trap (CHIP-TRAP) project, using SIMION software to simulate the transport of ions from ions sources to the trap. The beamline length was chosen to maintain a relatively compact system, while allowing separation of ions of different nominal *m*/*q* ratio via their time-of-flight. A picture of the simulated beamline and ions being transported is shown in Fig. 1.

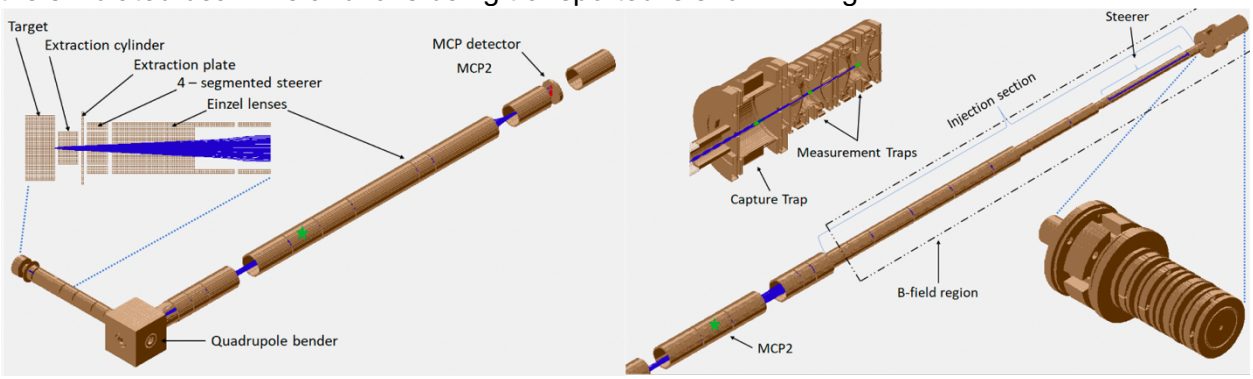

Figure 1: SIMION simulations of (left) the CHIP-TRAP beamline from the laser ablation ion source to microchannel plate 2 (MCP2), and (right) with MCP2 replaced by a drift tube so that ions travel to and enter the Penning traps.

After completing these simulations, we began work on the CAD design of beamline electrodes and vacuum housing. Figure 2 shows (a) a schematic CAD drawing of the beamline, (b) a close-up view of one of the einzel lenses used to focus the ion beam along its path, (c) the Bradbury Nielsen Gate (BNG) – see later text for description, and (d) one of the feedthroughs that places a Microchannel Plate (MCP) detector or transport lens in the path of the ion beam.

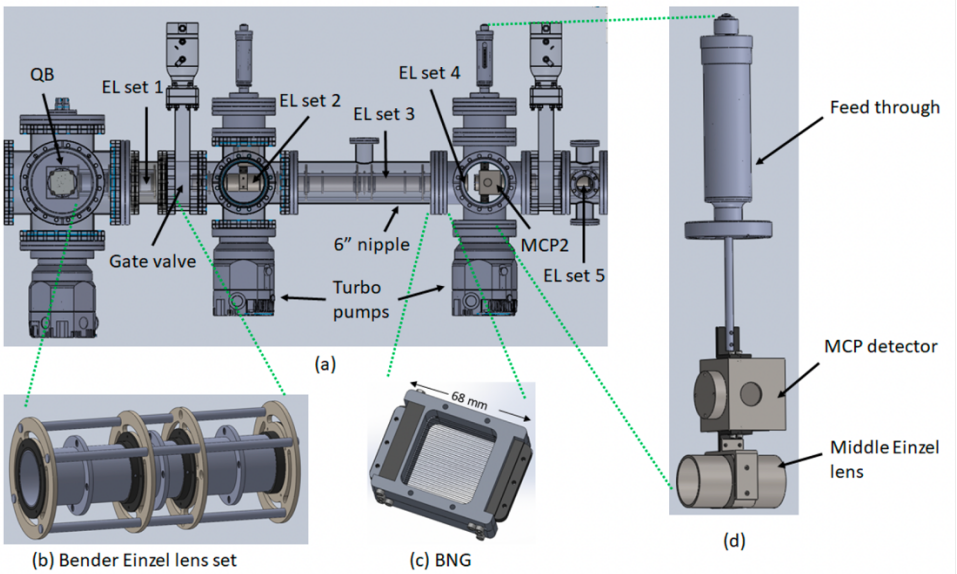

Figure 2: CAD drawing of (a) vacuum housing and beamline, (b) one of the einzel lenses, (c) the Bradbury Nielsen Gate (BNG), and (d) the feedthrough housing the Microchannel Plate (MCP) detector or transport lens.

Fabrication of the beamline components, such as the einzel lens in Fig. 2 (b) began in the machine shop in the CMU physics department. Other vacuum chamber components, gate valves, vacuum pumps, etc were ordered from external companies.

Before the beginning of this project we had already begun work on the design, fabrication, and assembly of a laser ablation ion source (LAS). During this period, we completed the assembly of the LAS in a test set-up and performed initial tests with it. A CAD drawing of the LAS showing the target and extraction electrodes can be seen in Fig. 3 (left) and a picture of the test set-up is shown in Fig. 3 (right). The inset of Fig. 3 (right) shows a picture of ions hitting the phosphor screen of the MCP.

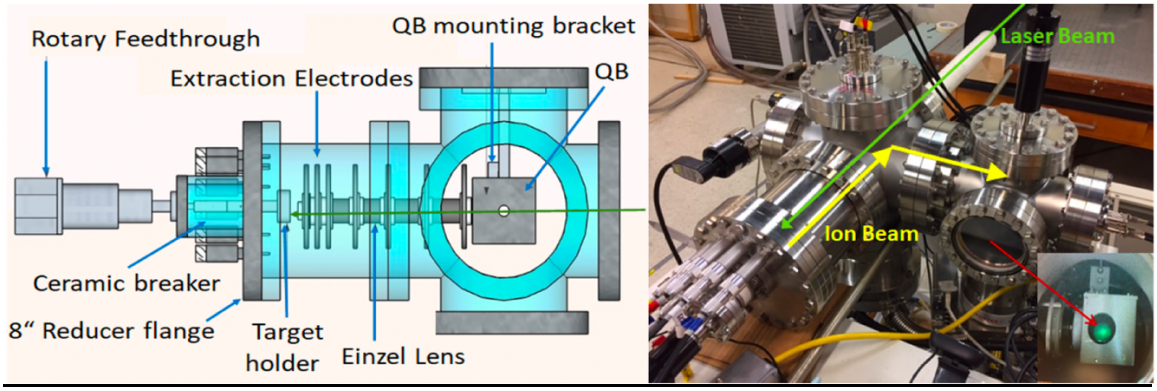

Figure 3: (Left) CAD drawing of the LAS showing the rotatable feedthrough and target holder, extraction electrodes, and vacuum beamline; (Right) Picture of the LAS test set-up and inset (bottom right) showing ions hitting the MCP.

Year 2 (Jul 2017 – Jun 2018):

During this year of the project, the CAD design was completed with the inclusion of a beam stand to allow alignment of the beamline in the x and y direction, so that it can be centered in the bore tube of the magnet, and the ability to have motion along the z direction to adjust the position of the Penning traps in the magnetic field.

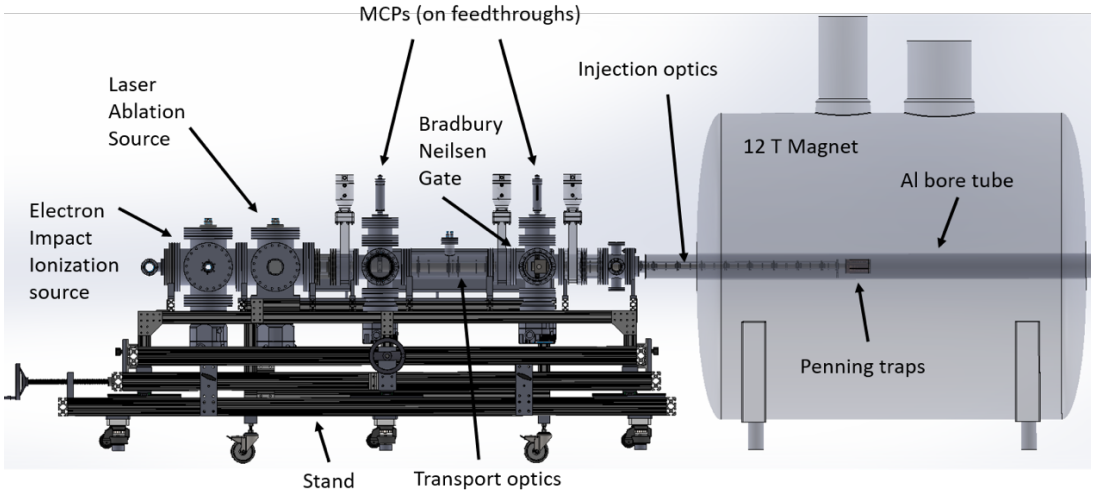

Figure 4: CAD drawing of the beamline stand and the ion sources, transport and injection sections of the beamline, and Penning traps housed in the 12T magnet.

We also designed and fabricated a Bradbury Nielsen Gate (BNG). The BNG can be used to deflect the path of ions so that they do not continue down the beamline. This is accomplished by applying opposite polarity voltages of ~several hundred volts to closely spaced (d = 1 mm) wires perpendicular to the beams path. When the voltage on the wires is at 0 V, relative to the beam energy, the ions pass through unimpeded. Hence, by fast switching (~100 ns) the BNG voltages off and back on, ions arriving at a particular time, corresponding to a particular m/q, can be allowed

to pass, while others are blocked. A schematic diagram showing the operation of the BNG is shown in Fig. 5 (left) and the CAD drawing of our BNG is shown in Fig. 5 (right).

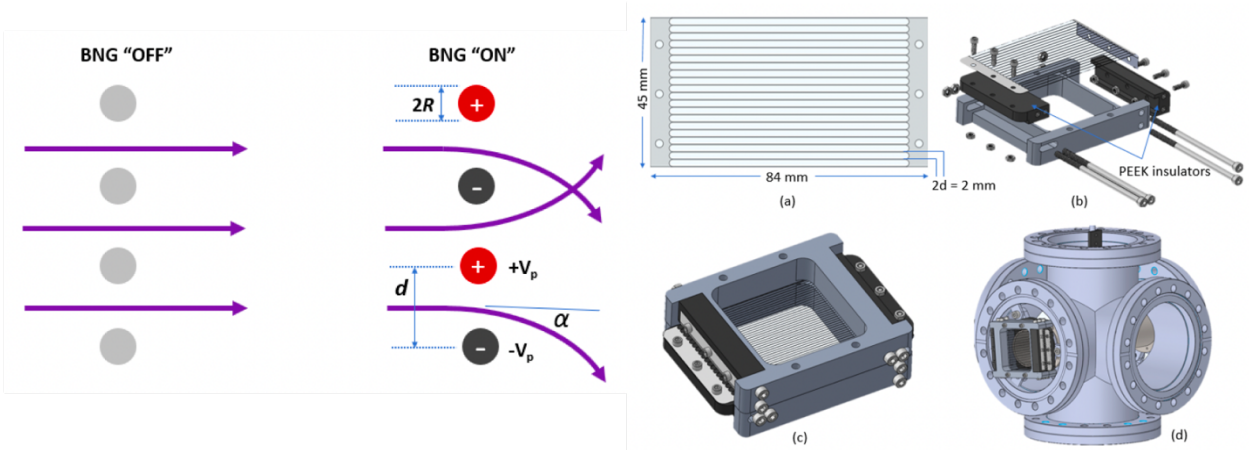

Figure 5: (Left) Operation of the BNG – with no voltage applied to the wires, ion pass through the BNG unimpeded; with opposite polarity voltages applied to adjacent wires, ions are deflected. (Right) CAD drawings of our BNG design and installation in a vacuum chamber in the beamline.

During this period we completed the commissioning and calibration of the LAS in the test set-up shown in Fig. 3 (right) above. This calibration employed a sigradur® glassy carbon target in the LAS to produce carbon cluster ions $^{12}C^+$, $^{12}C_2^+$, etc. Carbon clusters up to about $^{12}C_{12}^+$ were observed with identification via their time-of-flight (TOF). Fig. 6 (a) shows the count rate of the various $^{12}C_n^+$ peaks on the MCP vs their TOF. Fig. 6 (b) shows that TOF goes as $(m/q)^{1/2}$ as expected. The difference in the simulated vs predicted curves in the figure (where predicted is a fit to the TOF data vs $(m/q)^{1/2}$) is due to the initial energy distribution of the ions.

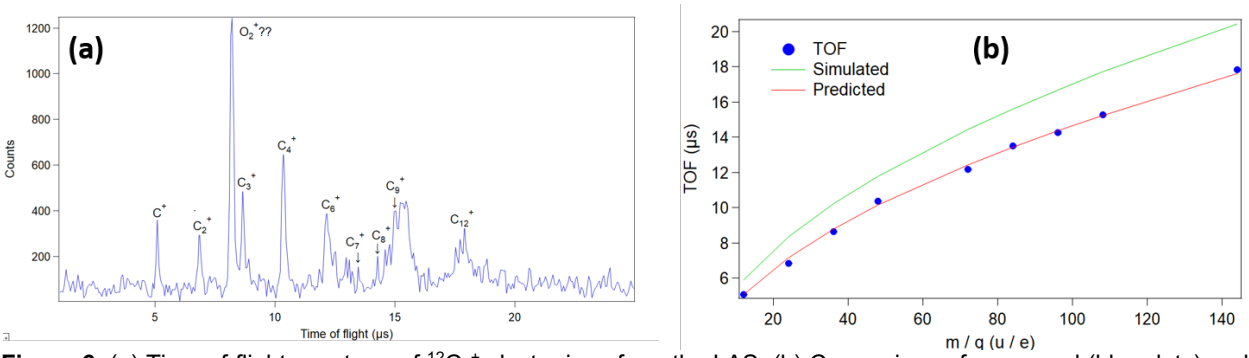

Figure 6: (a) Time-of-flight spectrum of $^{12}C_n^+$ cluster ions from the LAS. (b) Comparison of measured (blue dots) and simulated (green line) times-of-flight vs m/q.

During this period we also began simulations of ion motion in the Penning traps. CHIP-TRAP has a triple-trap structure. The first trap is a cylindrical geometry capture/preparation trap used to capture bunches of ions, remove contaminants, and prepare the ions for transfer to one of the two precision hyperbolic geometry measurement traps where simultaneous cyclotron frequencies comparisons will be performed with one ion in each of the two traps. The measurement traps were modeled on the LEBIT Penning traps and were designed in SolidWorks, see Fig. 7. The specialized measurement trap components were fabricated in the machine shop at the NSCL.

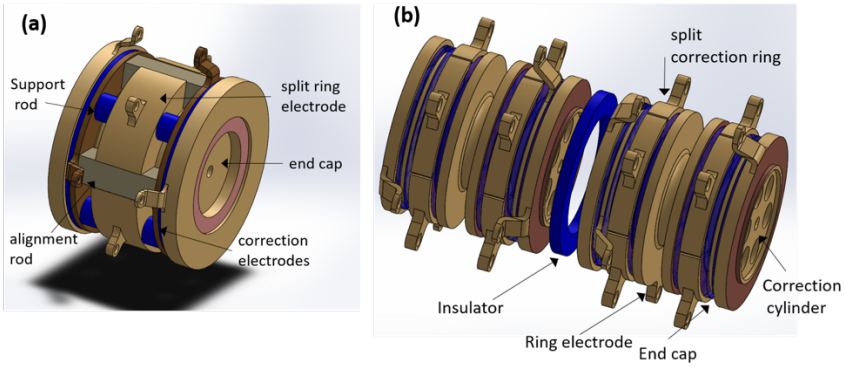

Figure 7: SolidWorks drawings of the CHIP-TRAP (a) capture/preparation Penning trap and (b) precision measurement Penning traps.

Year 3: (Jul 2018 – Jun 2019):

During this reporting period, the beamline stand was constructed and the beam transport electrodes were assembled in the vacuum beamline, which was installed on the beamline and commissioned. A picture of the completed beamline is shown in Figure 8.

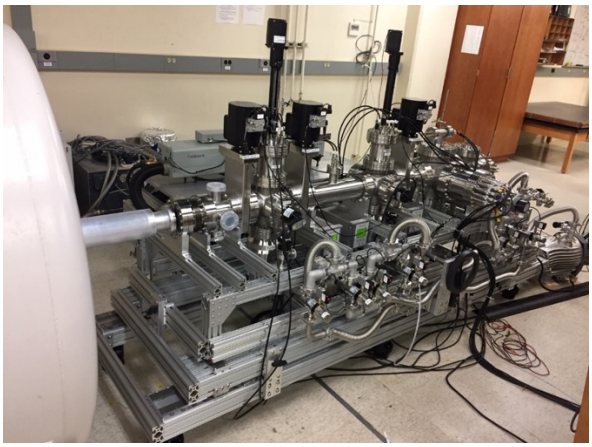

Figure 8: Picture of the assembled CHIP-TRAP beamline and 12 T magnet

The laser ablation ion source (LAS) was installed and commissioned on the main beamline (it had previously been tested on a test set-up). A Sigradur® glass carbon target was again used to produce $^{12}C_n^+$ clusters and calibrate the time-of-flight spectrum, see Figure 9.

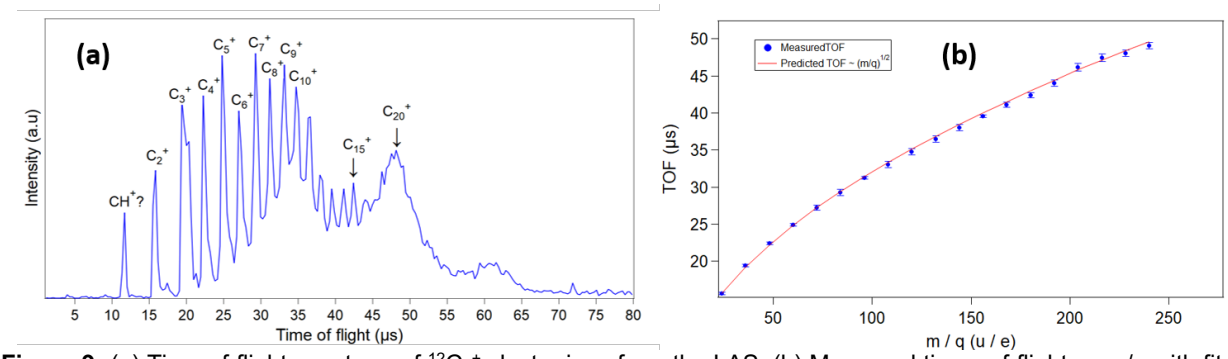

Figure 9: (a) Time-of-flight spectrum of $^{12}C_n^+$ cluster ions from the LAS. (b) Measured times-of-flight vs m/q with fit of expected behavior, $\mathrm{TOF} \propto \sqrt{m/q}$.

The production of ions from other metal targets was also investigated (e.g. Al, Ti, Zn, Ag, Au, W). In particular, we investigated the production of $^{165}Ho^{+}$ ions via ablation of small quantities of holmium deposited on the surface of different metal backings. To do this, holmium powder was dissolved in nitric acid and several ~50 μL drops of holmium nitrate solution, containing in total ~10^{17} – 10^{20} ^{165}Ho atoms (depending on the concentration used) were deposited and then dried out on the metal surface. This will mimic the technique we plan to use for the ^{163}Ho measurement for which ^{163}Ho must be synthetically produced at a reactor or accelerator facility, which can provide only small quantities of ^{163}Ho. It was found that Ti and W backing targets worked best in terms of the proportion of Ho^{+} vs HoO^{+} ions that were produced. We plan to use Ti, since the Ti^{+} ions that are also produced during the ablation process have a greater temporal separation from the Ho^{+} ions compared to that of W^{+} and Ho^{+}. Figure 10 shows a tungsten backing plate with drops of holmium nitrate solution dried out on it, and a time-of-flight spectrum showing $^{165}Ho^{+}$ ions produced with the LAS.

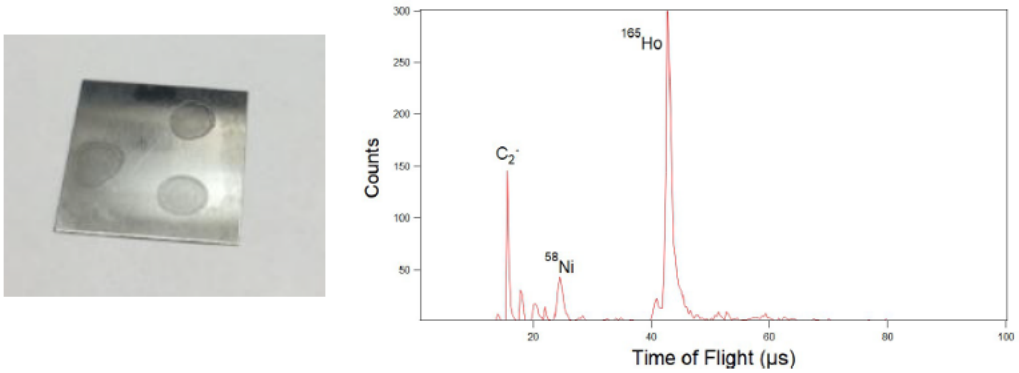

Figure 9: (Left) tungsten backing plate with drops of holmium nitrate solution dried out on it, (Right) a time-of-flight spectrum showing $^{165}Ho^{+}$ ions produced with the LAS using a nickel backing target.

The high-precision copper trap electrodes were fabricated at the National Superconducting Cyclotron Laboratory machine shop and received in Dec 2018. A picture of the assembled triple trap structure before gold plating is shown in Figure 10 (left). The electrodes were then sent out to a company for gold plating, see Figure 10 (right).

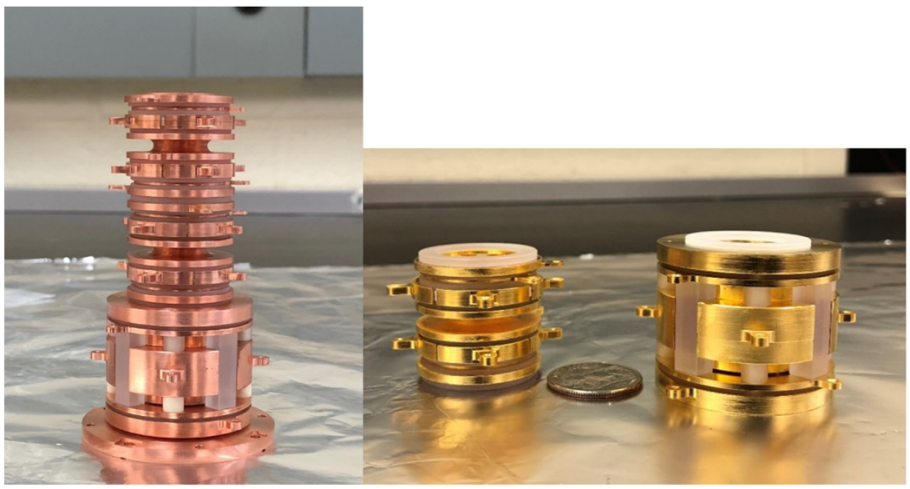

Figure 10: (Left) Assembled triple Penning trap structure of CHIP-TRAP before gold plating, consisting of a cylindrical capture trap (lower) and two hyperbolic precision measurement traps (upper), and (Right) One assembled hyperbolic trap (left) and the capture trap (right) after gold plating.

Year 4: (Jul 2019 – Jun 2020):

During this period, the Penning traps were gold plated and assembled, see Figure 10 (Right) above. The CAD design of the injection optics was completed, see Figure 11 (upper), and they were fabricated in the CMU machine shop. The injection optics were assembled and the capture trap and one of the precision measurement traps was installed on the end of the injection optics section, see Figure 11 (lower). The injection optics and trap assembly was installed in the bore of the 12 T magnet.

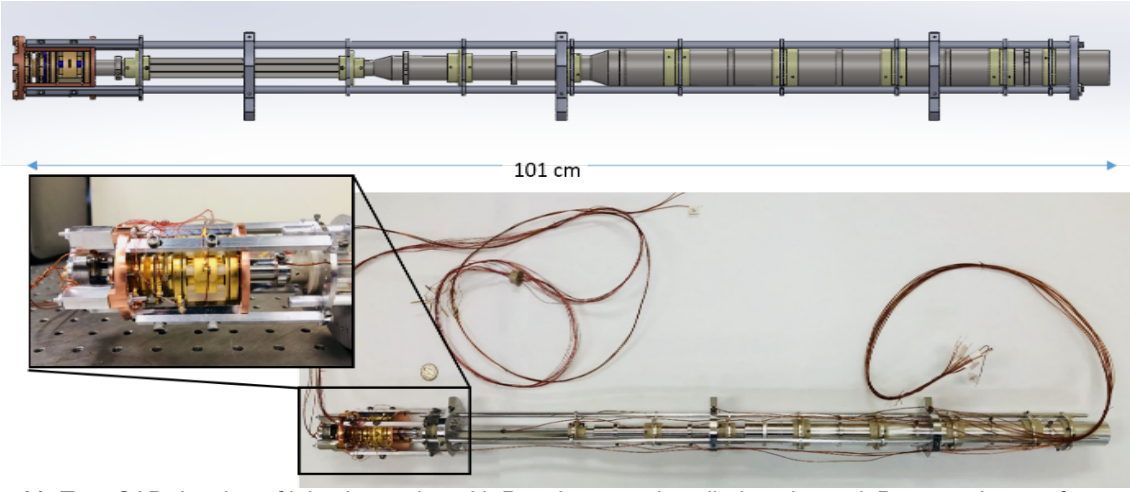

Figure 11: Top: CAD drawing of injection optics with Penning traps installed on the end. Bottom: picture of assembled injection optics and Penning traps, Inset: zoom in of Penning traps installed on end of injection optics in support frame. The thermal emitter is housed to the left of the Penning traps.

After installation of the Penning traps and pump down, ions were produced inside the capture trap by electron impact ionization of background gas using an electron beam that was produced by a thermal emitter and then passed through the trap. We were able to detect the magnetron and then cyclotron motion of ions in the trap by driving them with an rf pulse close to their resonant frequencies. Ions were detected via the image currents they induced in the trap electrodes using a low noise differential amplifier connected across two of the four quarters of the ring electrode. Figure 12 shows the detected ion signal after performing an FFT on the digitized time domain signal from the amplifier. The central peak is at the trap cyclotron frequency of the ion. The peaks to the right and left are the sum and difference frequencies of the trap cyclotron, f_+, and magnetron, f_-, frequencies, resulting from a non-zero magnetron amplitude of the ions i.e. $f_+ \pm f_-$. Based on the cyclotron frequency, the ion species is identified as H_3O^+.

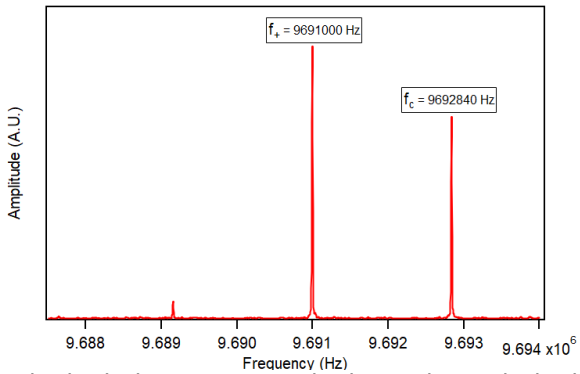

Figure 12: FFT of ion signal after production in the capture trap via electron impact ionization and excitation by a pulsed rf drive close to their trap cyclotron frequency. The central peak corresponds to the frequency of the trap cyclotron mode, while the peaks to the right and left are the sum and difference of the trap cyclotron and magnetron frequencies.

During this reporting period, we also commissioned a Penning ion trap source. This source uses a thermal electron emitter to ionize gas inside a cylindrical Penning trap electrode structure housed inside a permanent rare earth ring magnet (B ~0.55 T). Ions are released from the trap in a bunch by lowering the voltage on one of the end caps. A CAD drawing and picture of the PIT source is shown in Figure 13.

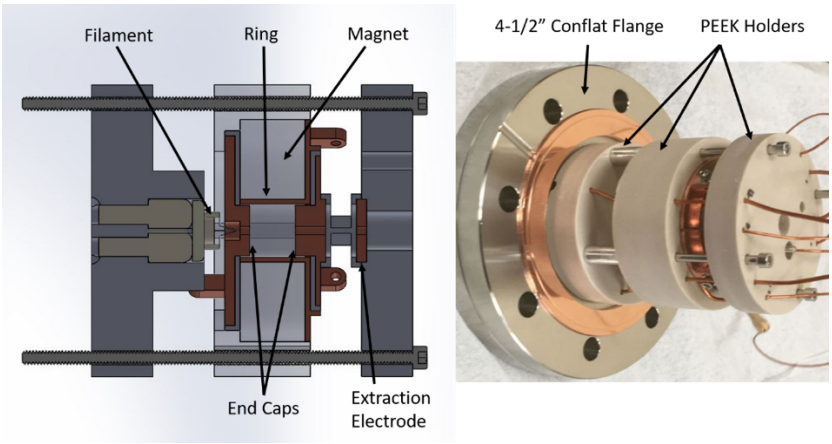

Figure 13: (Left) CAD drawing of PIT source, (Right) picture of PIT source after assembly on a vacuum flange.

The Penning ion trap source was successfully used to produce bunches of ions and transport them along the CHIP-TRAP beam line to the MCP detector. A plot of counts vs time after the PIT source end cap is lowered can be found in Figure 14, which shows the temporally grouped arrival of ions. Ions were produced by ionizing background gas in the trap and an initial identification as H_3O^+ was made based on a shorter time peak thought to be H^+, H_2^+, or He^+.

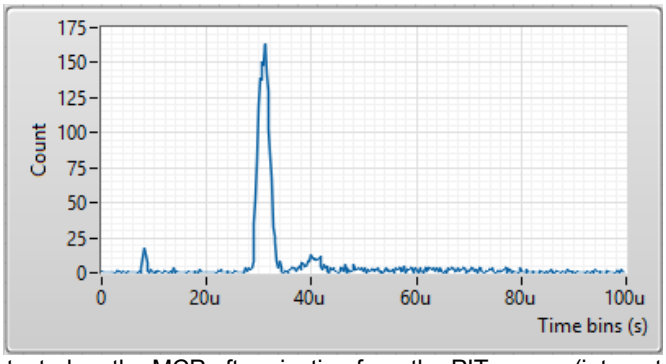

Figure 14: Ion bunch detected on the MCP after ejection from the PIT source (integrated over ~10s of cycles).

Year 5: (Jul 2020 – Dec 2021):

During this period, commissioning of the capture trap was continued, and was used to map out the B-field of the magnet in the region that the trap is housed. This was done by measuring the cyclotron frequency of ions in the trap as a function of radius, and by measuring the cyclotron frequency of ions in the trap (with fixed radius) as a function of trap position – by moving the beamline bore tube through the magnet using the translatable beam stand. Data from these measurements is shown in Figure 15.

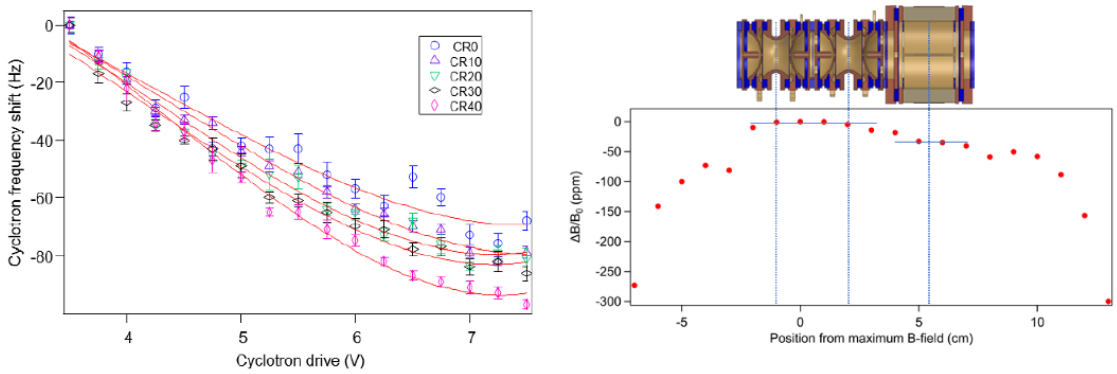

Figure 15: (Left) Cyclotron frequency as a function of radial amplitude in the trap. (Right) Cyclotron frequency converted to fractional magnetic field shift vs axial position along magnet bore and relative location of traps in the magnet bore.

Further commissioning of the PIT was performed by leaking different gasses into the PIT ionization/trapping region. He and Ar gas were used, resulting in peaks in the TOF spectrum on the MCP at the expected times for these ions. From these data a calibration plot of $(m/q)^{1/2}$ vs TOF was made and the residual ion peak (ions made by ionizing residual gas in the PIT) was identified as H_3O^+.

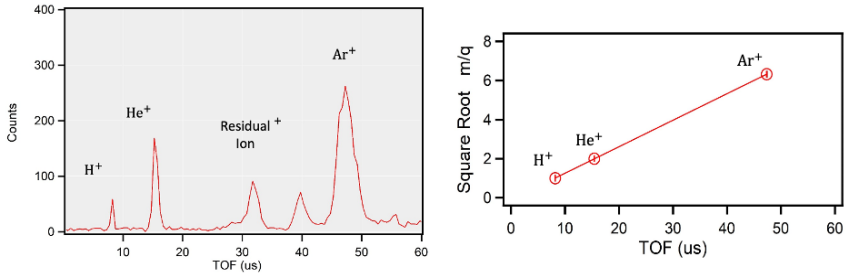

Figure 16: (Left) TOF spectrum for ions released from PIT source after He and Ar gas was injected in the PIT. (Right) Calibration plot of $(m/q)^{1/2}$ vs TOF, which enabled identification of residual ions (made from background gas) as H_3O^+.

Further work was undertaken with the LAS to test the production of Mg^+ production from a solution of MgHCl that was dried out on a metal backing target. The goal was to mimic the production of Be^+ ions from a solution of BeHCl (without the need to use beryllium), with an ultimate goal of making $^7Be^+$ ions from a ^{7}BeHCl solution available from the National Isotope Development Center. A measurement of $^7Be^+$ vs $^7Li^+$ with CHIP-TRAP to <0.1 eV will enable a precise determination of the ^{7}Be EC decay Q value to test systematics and aid in the analysis of the BeEST experiment to search for the signature of sterile neutrinos in ^{7}Be EC decay.

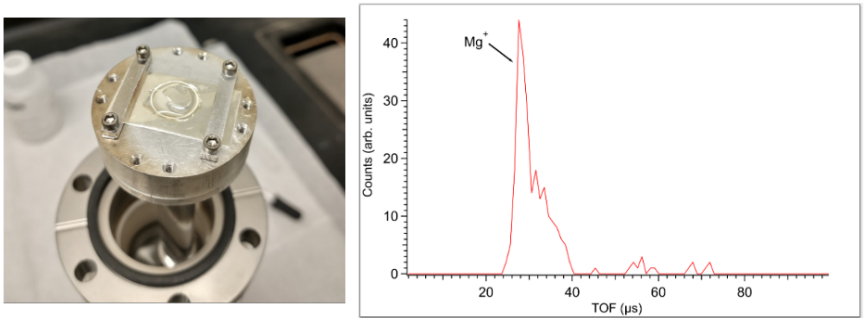

Figure 17: (Left) LAS backing target with MgHCl solution dried out on it, (Right) TOF spectrum produced from MgHCl target. The main peak is identified as Mg^+ from the TOF calibration.

During this period we also completed the fabrication and assembly of a Multi-Reflection Time-of-Flight Mass Separator (MR-TOF-MS), shown in Figure 18 (Left). This began as the MPhys project of a visiting undergraduate MPhys student from University of Surrey, UK, and is being continued as part of the Ph.D. thesis of Ramesh Bhandari. The MR-TOF-MS was installed in the CHIP-TRAP beamline and initial commissioning began toward the end of 2021. Figure 18 (Right) shows the SIMION workbench used to simulate the transport of ions into the MR-TOF-MS. These simulations were used in the initial design phase of the MR-TOF-MS, which was based on the Notre Dame set-up, and then to investigate optimal voltages for confining ions in the MR-TOF. Simulations showed that a resolving power of ~25,000 – 30,000 should be achievable with this apparatus. This, in combination with the BNG described earlier, will enable us to temporally separate ions of different *A/q* before they enter the magnet to be captured in the Penning trap. Separation of some isomers of nominally the same *A/q*, e.g. $^{40}K^{+}$ and $^{40}Ca^{+}$ could be performed with the achievable resolving power. Initial results show that ions can be captured in the MR-TOF-MS for several cycles, then be released and detected on the MCP with a similar FWHM to the ion distribution of ions that pass straight through the MR-TOF-MS.

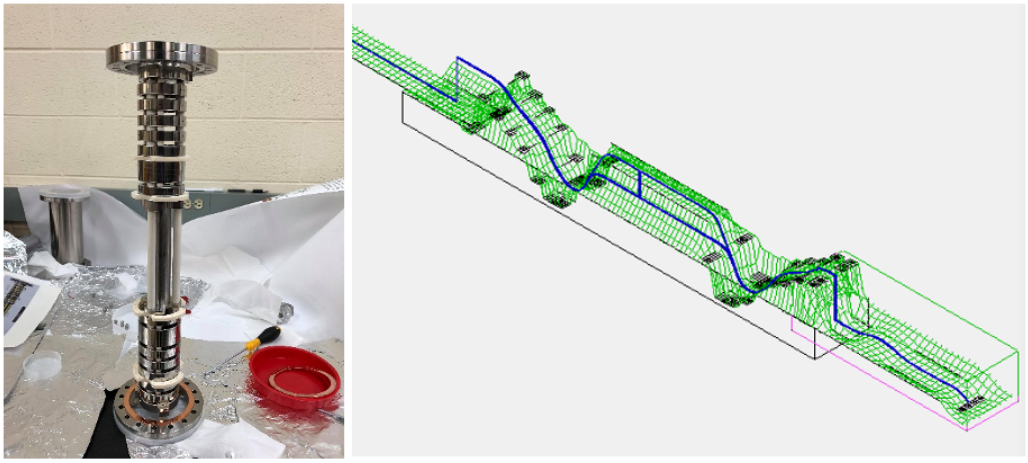

Figure 18: (Left) Assembled MR-TOF-MS before installation in the CHIP-TRAP beamline. (Right) SIMION simulation of ions entering the MR-TOF-MS, being confined for a number of cycles, then being released and reaching the MCP.

The MR-TOF-MS will increase the resolving power of the time-of-flight section of the CHIP-TRAP beamline that is used to temporally separate ions of different A/q before they enter the magnet to be captured in the Penning trap. This will enable an increase in efficiency and sensitivity.

Finally, in this period we designed and built a test stand for the Penning trap cryocooler, see Figure 19. The cryocooler will be used to cool the Penning traps and associated ion detection electronics down to ~4.2 K. This will reduce thermal noise in the detection electronics that would otherwise limit the ability to detect single ions in the trap, and it will improve the vacuum inside the Penning traps enabling longer trapping times, leading to higher achievable precisions. The cryocooler was installed and turned on and found to be operating as expected. Future tests will involve measuring the cool down time and cooling down the cryogenic amplifier.

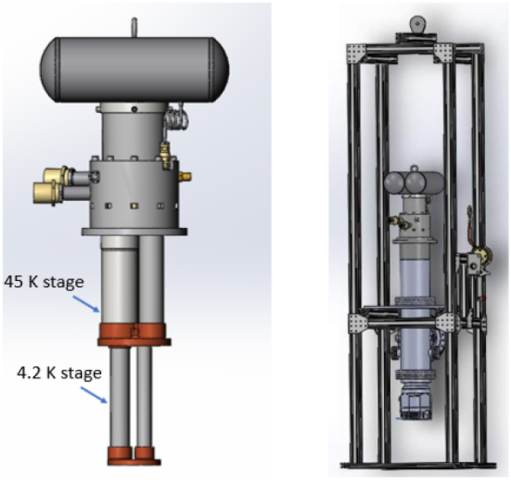

Figure 19: (Left) CAD drawing of the cryocooler. (Right) CAD drawing of the crycooler attached to the vacuum test chamber on the test stand.

B) Ultra-low Q value β-decay measurements

(i) Online measurements at Argonne National Laboratory

Measurements of the β-decay Q values of ^{115}Cd, ^{112,113}Ag were performed at the Canadian Penning Trap (CPT) facility at Argonne National Laboratory (ANL) during October 2016 by Ph.D. students Rachel Sandler and Nadeesha Gamage and the PI in collaboration with the CPT group. The initial analysis of the data showed up to ~10 keV systematic shifts in the data when comparing our test ratio measurements of precisely known masses $^{112}Sn^{+}/^{112}Cd^{+}$ and $^{115}In^{+}/^{115}Sn^{+}$ with literature values, and systematic shifts of several keV when taking data with different measurement times for the same ratio. This effect was studied by the CPT group in January 2017 and some additional data for ^{115}Cd was obtained. These data were analyzed (by the CPT group and at CMU) to understand/model the systematic shift and correct the data for it. The cause of the systematic effect observed in the original data was found to be due to residual magnetron motion of the ions in the trap after loading. We were able to model this effect, parameterize it, and use the model to correct the ^{115}Cd data. Corrected data from the 2016 run, along with data from the 2017 run with ^{115}Cd is shown in Figure 20.

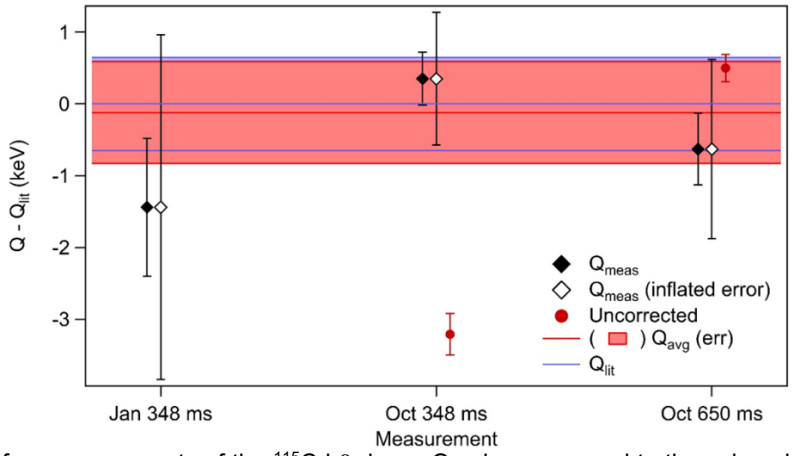

Figure 20: Results for measurements of the ^{115}Cd β-decay Q value compared to the value obtained from AME data. Red circles are the two data sets obtained in the Oct 2016 run that suffered from a systematic effect. Black diamonds show the data from the Jan 2017 run for which the systematic effect was accounted for and the Oct 2016 runs after using our model to correct the data. The white diamonds include an estimate of the uncertainty in the systematic correction. The red line and shaded region show our average result and its uncertainty while the blue lines show the AME value (the zero line) and associated uncertainty.

We also used our model to estimate systematic uncertainties for the ^{112,113}Ag data. While the model of the systematic shifts applies to all ions studied, the parameters used to correct the ^{115}Cd data were obtained using ^{115}Cd data, so were not used to attempt to correct the ^{112,113}Ag data. We determined the Q values for the ultra-low Q value decay branches of these isotopes to be -1.2(2.2) keV for ^{112}Ag and 67.4(3.9) keV for ^{113}Ag. Hence, ^{113}Ag is ruled out, but further data was needed for ^{112}Ag

A third experimental run took place in November 2018 with three additional days of beam time at CPT/ANL. We took additional data for ^{115}Cd and ^{112}Ag (it was deemed unnecessary to take additional data for ^{113}Ag since our previous result completely ruled out the possibility of an ultra-low decay branch). Analysis of the data was performed by graduate student, Rachel Sandler, as part of her PhD thesis (graduation Fall 2019). However, shortly afterwards, an additional systematic was discovered at CPT. A second graduate student, Nadeesha Gamage, reanalyzed the data in Fall 2020/Spring 2021 and wrote up the results in a paper that was submitted to Physical Review C in February 2022. The final results are summarized in Figure 21 and Table I. The ground-state to ground-state Q values for ^{112}Ag and ^{115}Cd are in agreement with those obtained from the AME data, but are factors of 11 and 2 more precise, respectively. The Q value for ^{113}Ag showed a 69(17) keV shift compared to the AME value, and is a factor of 4 more precise.

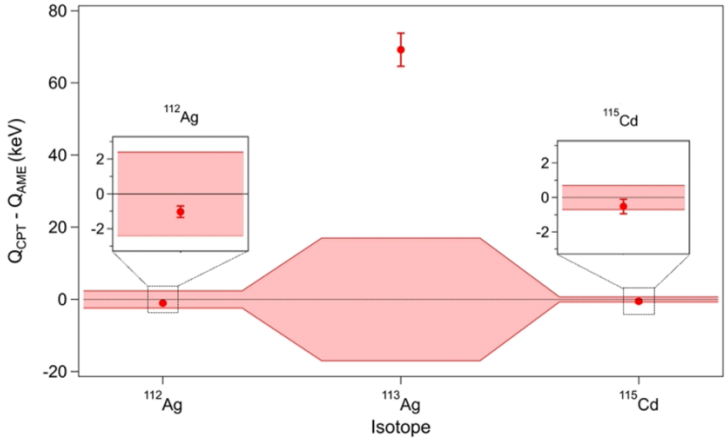

Figure 21: Ground-state to ground-state Q values measured at. CPT. The red bands show the AME2020 uncertainty and the red dots are our measured values.

The potential ultra-low Q value branch for ^{112}Ag was determined to have an energy of -7.6(3) keV, indicating that this branch is not energetically allowed. For ^{115}Cd it was determined to be 2.6(3) keV, indicating that it is not ultra-low (<1 keV). For the ^{113}Ag decay branch to the ½$^+$ state at 2105.6 keV in ^{113}Cd, which was originally under investigation, the Q value was found to be 70(5) keV. However, there is the possibility now of a potential decay to another ½$^+$ state in ^{113}Cd at 2080(10) keV with a Q value of 6(11) keV, where the uncertainty is dominated by the uncertainty in the energy of the ½$^+$ state. Hence, a more precise measurement of this energy level is needed to further evaluate this potential decay branch.

Table 1: Q values for potential ultra-low Q value decays. The Q_{UL} values were obtained using the gs–gs Q values shown in Figure 21, and excited state energies, E^*, from the NNDC. All values listed are in keV.

Decay	E^*	Q_{UL}	
		CPT	AME
^{112}Ag → ^{112}Cd	3997.75(14)	-7.59(26)	-6.6(2.4)
^{113}Ag → ^{113}Cd	2015.6(2.5)	70.1(5.2)	0.9(16.8)
	2080(10)	5.7(11.0)	-63.5(19.4)
^{115}Cd → ^{115}In	1448.787(9)	2.57(34)	3.1(0.7)

(ii) Measurements at the National Superconducting Cyclotron Laboratory

^{139}La β-decay Q value: During 2017 we performed a measurement of the mass of ^{139}La using the Low Energy Beam and Ion Trap (LEBIT) facility at the NSCL. This measurement was led by Ph.D. student Rachel Sandler in collaboration with the LEBIT group. Our result was combined with the atomic mass of ^{139}Ba from AME data (given to 0.32 keV) to obtain the ground-state to ground-state Q value of 2308.4(7) keV. Comparison with nuclear energy level data for the daughter, ^{139}La, showed that the Q value for the potential ultra-low Q value decay to the 2313(1) keV (J^{π} unknown) state is -4.6(1.2) keV and to the 2310 keV ($1/2^{+}$) state is -1.6(19.0) keV, where the number in parentheses includes the uncertainty in the energy of the final state. Hence, an ultra-low Q value decay to the 2313 keV level is ruled out, while more precise data for the energy of the 2310 keV level is required.

In 2018, we performed a measurement of the mass of ^{89}Y to combine with the mass of ^{89}Sr from the AME, which is given to a precision of 0.09 keV. We hence obtained the ^{89}Sr ground-state to ground-state Q value, which we determined to be 1502.2(4) keV. Therefore, we found that the Q value for a potential ultra-low Q value decay of ^{89}Sr to the 1507.4(1) keV ($3/2^{-}$) state in ^{89}Y is -5.2(4) keV, ruling out such a decay for ^{89}Sr as not being energetically allowed. The results of these measurements for ^{89}Sr and ^{139}Ba were published in Physical Review C in 2019.

^{75}Se and ^{75}Ge β and EC decay Q values: In 2019, we submitted a proposal to the special NSCL-ReA PAC for a measurement of the mass of ^{75}As with the goal of precisely determining the ^{75}Se – ^{75}As electron capture, and the ^{75}Ge – ^{75}As β-decay Q value to evaluate potential ultra-low Q value decay branches in these isotopes, as shown in Figure 22. Using atomic mass data from the AME and nuclear energy level data from the NNDC, the potential ultra-low Q value branches had energies of –0.7(1.0) keV for ^{75}Se and 5.2(1.1) keV for ^{75}Ge. The uncertainty in the Q value is dominated by the 0.88 keV/c^2 uncertainty in the mass of ^{75}As. The atomic masses of ^{75}Se and ^{75}Ge on the other hand are already known to precisions of 73 eV/c^2 and 52 eV/c^2, respectively. This proposal was approved and the experiment ran in December 2021. The analysis is still underway, but preliminary results indicate the potential ultra-low Q value β-decay branch for ^{75}Ge is not energetically allowed, but that the potential ultra-low Q value electron capture decay branch for ^{75}Se has an energy of around 1 keV, making it an interesting candidate for further study.

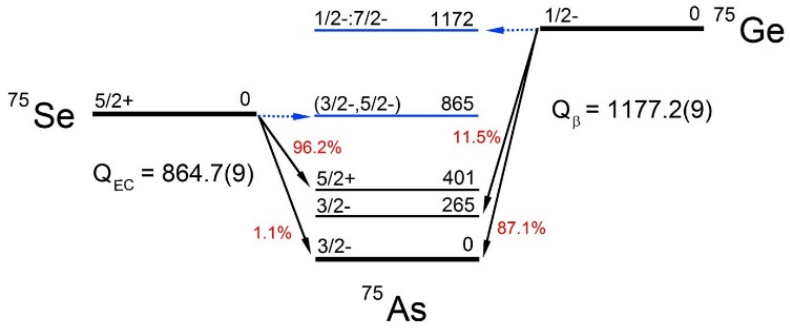

Figure 22: Level scheme showing potential ultra-low Q value branches of ^{75}Se and ^{75}Ge to excited states in ^{75}As.

As part of this project, we performed an analysis of all β-decay and electron capture decay candidates across the nuclear chart, evaluating ground-state to ground-state Q values using data from the AME, and searching for potential ultra-low Q value decay branches using data from the NNDC. We found ~100 candidates, including ^{75}Se, ^{75}Ge, ^{89}Sr, ^{112,113}Ag, and ^{139}Ba that we have investigated at ANL/CPT and NSCL/LEBIT, and others that have been investigated by other groups. This study was published as a conference proceeding paper in Hyperfine Interactions in 2019. We have recently completed an updated study using data from the most recent 2020 AME, which was submitted to Physical Review C in January 2022.

C) β-decay and double β-decay Q value measurements

(i) Measurement of ^{138}La and ^{176}Lu β-decay Q values at the NSCL

In 2017/2018, we took data to determine the ^{138}La – ^{138}Ce β-decay Q value, the ^{138}La – ^{138}Ba electron capture Q value, and the ^{138}Ce – ^{138}Ba double electron capture Q value at the LEBIT facility. These measurements were led by Ph.D. student Rachel Sandler in collaboration with the LEBIT group. We have found the ^{138}La β-decay Q value to be 1052.42(41) keV and the ^{138}La EC Q value to be 1748.41(34) keV. After subtracting the energy of the 788.74(1) keV (2^+) daughter state in ^{138}Ce, our β-decay Q value of 263.68(41) keV is in excellent agreement with the β-decay spectrum end-point energy measurement of 264.0(4.3) keV, performed by Quarati, *et al*. using $LaBr_3$ detectors, but is a factor of almost 10 more precise, see Figure 23 (left). We collaborated with theorist, Xavier Mougeot from Laboratoire National Henri Becquerel, France, to perform calculations of the β- spectrrum shape factor and of the EC probability ratios. Using our new Q value, uncertainties in the experimental shape factor for the ^{138}La β-decay spectrum are reduced by an order of magnitude compared to those found using the Q value obtained from the AME 2016 mass values, see Figure 23 (right).

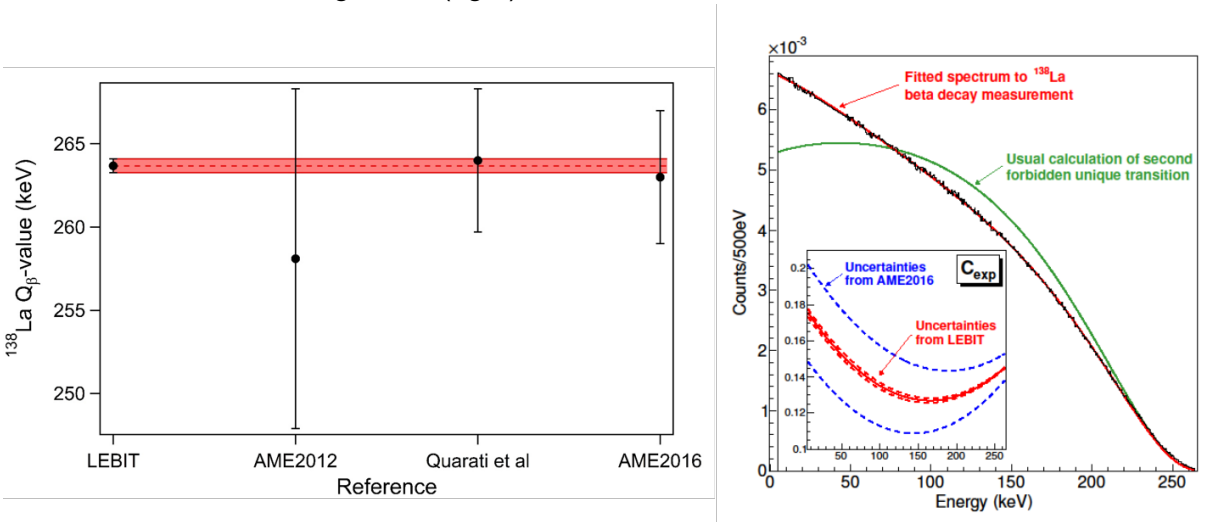

Figure 23: (Left) Measurement of the ^{138}La β-decay Q value (data point marked LEBIT and red shaded band) compared with results from the 2012 and 2016 Atomic Mass Evaluations (AMEs), and a measurement of the end-point energy of the ^{138}La β-decay spectrum by Quarati et al. (Right) ^{138}La β-decay spectrum: data from Quarati *et al*. (black lines); usual theoretical calculation (green line), fitted spectrum (red line) obtained by multiplying usual calculation by experimental shape factor, C_{exp}, shown in the inset.

Uncertainties in the calculated EC probability ratios are reduced by factors of 2 – 3 using our new EC Q value compared to using the value obtained from AME 2016 data. In addition, agreement between the calculated and experimental values for the L/K shell capture ratio is significantly improved when using our new Q value, see Table II. The results of this measurement and study was published in Physical Review C in 2019.

Table 2: Influence of the Q value (from AME 2016 or from our measurement at LEBIT) on the theoretical predictions of the capture probability ratios for ^{138}La compared to experimental values.

EC ratio	Experiment	AME2016	LEBIT
L/K	0.391(3)	0.403(8)	0.3913(26)
M/K	0.102(3)	0.0996(24)	0.0964(10)
M/L	0.261(9)	0.247(8)	0.2464(30)

Our collaboration with Mougeot and Quarati continued with a study of the β-decay and the (as yet unobserved) electron capture decay of ^{176}Lu (see decay scheme in Fig 24). Quarati *et al*. have performed precise measurements of the ^{176}Lu β-decay spectrum using LuAg:Pr scintillation detectors (and have also used these detectors to search for the 5th forbidden ^{176}Lu electron capture decay). At LEBIT we performed precise measurements of the ^{176}Lu – ^{176}Hf β-decay Q value, the ^{176}Lu – ^{176}Yb electron capture Q value, and the ^{176}Yb – ^{176}Hf 2β-decay Q value. Again, precise theoretical calculations of the β-spectrum were performed by Mougeot.

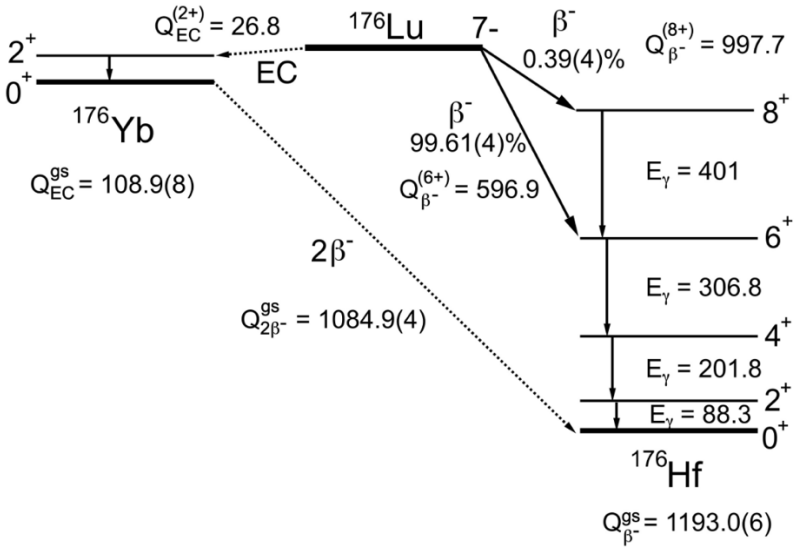

Figure 24: Decay scheme for Lu-Hf-Yb A = 176 triplet. Solid arrows indicate the observed 1st forbidden non-unique β-decays of ^{176}Lu, and dotted arrows indicate the energetically allowed, but as yet unobserved 5th forbidden non-unique EC decay of ^{176}Lu, and the double β-decay of ^{176}Yb.

Our measurement provided precise Q values of 1193.0(6) keV and 108.9(8) keV for the ^{176}Lu β-decay and EC decay, respectively. Combined with the energies of the 6$^+$ and 8$^+$ states in ^{176}Hf, the end point energies for the primary and secondary β-decays were determined to be 596.2(6) keV and 195.3(6) keV, respectively. These are in excellent agreement with the values 596.6(9) keV and 195.7(2.5) keV, obtained from Kurie plots of the two ^{176}Lu β-decay branches. The more precise Penning trap Q value determinations could then be used to more precisely constrain the form of the shape factors that were fitted to the experimental β-spectra. These results are reported in a paper that is currently being prepared for submission to Physical Review C.

(ii) Measurement of the ^{48}Ca single β-decay Q value.

^{48}Ca is a well-known double β-decay isotope of particular interest for having the highest double β-decay Q value and for the fact that it is also unstable against single β-decay. However, the 5th forbidden single β-decay mode has not been observed. To evaluate the feasibility of observing ^{48}Ca single β-decay, which would provide an interesting test of the underlying nuclear models used to describe ^{48}Ca single and double β-decay, a more precise determination of the mass of the single β-decay daughter, ^{48}Sc, is required (current uncertainty is ~5 keV/c^2). In 2018 we submitted a proposal to measure the mass of ^{48}Sc with the TITAN Penning trap facility at TRIUMF. This proposal was recommended for beam time in 2019. However, it was not possible to schedule the experiment in the 2019 cycle, and other Covid-related delays have further delayed the scheduling of this experiment.

(iii) Measurement of the ^{7}Be electron capture decay Q value.
In 2019 we began a collaboration with Kyle Leach of the BeEST experiment to perform a more precise determination of the ^{7}Be electron capture Q value. The BeEST (Berylium Electron capture in Superconducting Tunneling junctions) experiment aims to perform a precise measurement of the recoil energy of ^{7}Li after ^{7}Be electron capture (EC) decay in order to set limits on the mass of possible sterile neutrinos via decay kinematics. The Phase I run with the BeEST determined the recoil energy to 1 meV (future improvements could reach as low as 10 μeV). Using the current ^{7}Be EC decay Q value obtained from the most recent Atomic Mass Evaluation, which has an uncertainty of 71 eV, the calculated ^{7}Li recoil energy for zero neutrino mass is 9 meV. Hence, an improved Q value is immediately necessitated. In collaboration with the LEBIT group, Leach and I submitted a proposal to the 2019 NSCL-ReA PAC to perform a measurement of the ^{7}Be Q value to 1 eV. This would provide an uncertainty in the calculated recoil energy of 0.13 meV. This result would provide an important check of systematics in the BeEST experiment and will be used in the data analysis to extract upper limits on sterile neutrino masses. This experiment ran in October 2021. We were able to achieve a statistical precision of around 30 eV and are currently evaluating potential systematic uncertainties in the measurement. Although the statistical precision is worse than we aimed for in our proposal, the measurement still provides an increase in precision in the Q value, and hence, ^{7}Li recoil energy, of ~2. Moreover, it provides the first direct measurement of this Q value via atomic mass data. Future improvements in the ^{7}Be EC Q value will be required for the BeEST, which we intend to perform with CHIP-TRAP.

Other work supported by this project
During the course of this funded project, the PI maintained strong working collaborations with the LEBIT group at NSCL/FRIB. This involved engaging with collaborators in weekly meetings, and participating in experiments and other projects at the NSCL. The author participated in the preparation, operation and/or analysis of five online experiments with LEBIT at NSCL during this funding period, resulting in co-authorship on five regular journal articles, and one conference proceeding.

Student Tracking Information
During the course of this funding, four Ph.D. students, two Master's students, and one undergraduate student have worked on this project.

Table 3: Student Tracking Information

Student	Date Entered Grad School	Date Joined Group	Degree Program	Date Degree Awarded/ (Expected)	Advisor
Nadeesha Gamage	Aug 2014	May 2015	Ph.D.	Dec 2020	Redshaw
Rachel Sandler	Aug 2016	Sep 2016	Ph.D.	Dec 2019	Redshaw
Madhawa Horana Gamage	Aug 2016	May 2017	Ph.D.	May 2023	Redshaw
Jayani Dissanayaki	Aug 2016	Sep 2018	M.S.	Dec 2019	M. Horoi
Ramesh Bhandari	Aug 2017	Sep 2017	M.S.	Aug 2019	Redshaw
Ramesh Bhandari	Aug 2017	Sep 2017	Ph.D.	Aug 2023	Redshaw

Dissemination of Results

During the course of this funded project, the PI and his immediate research group published three regular journal articles, and two conference proceedings. The PI collaborated with the LEBIT group on five additional regular journal articles and one conference proceeding. Two additional articles have been submitted, and one further article is in preparation.

Regular journal articles (CMU group):

(1) R.M.E.B. Kandegedara, *et al.*, *β-decay Q values among the A = 50 Ti-V-Cr isobaric triplet and atomic masses of ^{46,47,49,50}Ti, ^{50,51}V, and $^{5-,52-54}$Cr*, Phys. Rev. C **96**, 044321 (2017).

(2) R. Sandler, *et al.*, *Direct determination of the ^{138}La β-decay Q value using Penning trap mass spectrometry*, Phys. Rev. C **100**, 014308 (2019).

(3) R. Sandler, *et al.*, *Investigation of the potential ultralow Q-value β-decay candidates ^{89}Sr and ^{139}Ba using Penning trap mass spectrometry*, Phys. Rev. C **100**, 024309 (2019).

Peer reviewed conference proceedings (CMU group):

(4) M. Horana Gamage, *et al.*, *Design and characterization of ion sources for CHIP-TRAP*, Hyperfine Interactions **240**, 93 (2019).

(5) N.D. Gamage, *et al*, *Identification and investigation of possible ultra-low Q value β decay candidates*, Hyperfine Interactions 240, 43 (2019).

Regular journal articles (in collaboration with LEBIT group):

(6) A. A. Valverde, *et al*., *High-Precision Mass Measurement of ^{56}Cu and the Redirection of the rp-Process Flow,* Physical Review Letters **120**, 032701 (2018).

(7) W.-J. Ong, *et al*., *Mass Measurement of ^{51}Fe for the determination of the ^{51}Fe(p,γ)^{52}Co reaction rate,* Physical Review C **98**, 065803 (2018).

(8) E. Leistenschneider, *et al.*, *Precision Mass Measurements of Neutron-Rich Scandium Isotopes Refine the Evolution of N=32 and N=34 Shell Closures,* Physical Review Letters **126**, 042501 (2021).

(9) J. Surbrook, *et al., First Penning trap mass measurement of ^{36}Ca*, Physical Review C **103**, 014323 (2021).

(10) Z. Meisel, *et al., Improved nuclear physics near A = 61 refines urca neutrino luminosities in accreted neutron star crusts*, Physical Review C **105**, 025804 (2022).

Peer reviewed conference proceedings (in collaboration with LEBIT group):

(11) J. Surbrook, *et al., Precision mass measurements of ^{44}V and ^{44m}V for nucleon-nucleon interaction studies*, Hyperfine Interactions **240**, 65 (2019).

Submitted journal articles (CMU group):

(1) D.K. Keblbeck, *et al*., *Updated evaluation of potential ultra-low Q value β-decay candidates*, submitted to Physical Review C (January 2021).

(2) N.D. Gamage, *et al*., *Precise Q value measurements of ^{112,113}Ag and ^{115}Cd with the Canadian Penning trap for evaluation of potential ultra-low Q value β-decays*, submitted to Physical Review C (February 2022).

Journal articles in preparation (CMU group):

F.G.A. Quarati, *et al.,* Measurements and computational analysis on the natural decay of ^{176}Lu, to be submitted to Physical Review C.

During the course of this funded project, the PI and his immediate research group have presented their results at various national and international conferences and seminars as invited and contributed talks and posters:

Invited seminars (Redshaw):

(1) Precise Atomic Mass Measurements for Neutrino Physics, NSCL Nuclear Science Seminar, January 18th 2017, Michigan State University, East Lansing, MI.
(2) Precise Atomic Mass Measurements for Neutrino Physics, Albion College Physics Seminar, February 10th 2017, Albion College, Albion, MI.
(3) Precise Atomic Mass Measurements for Neutrino Physics, Physics Division Nuclear Science Seminar, April 17th 2017, Argonne National Laboratory, IL.
(4) Precise Atomic Mass Measurements for Nuclear and Neutrino Physics, Mines Fundamental Physics Seminar, Oct 1st 2019, Colorado School of Mines, Golden, CO.
(5) Searches for ultra-low Q value beta-decay candidates using Penning trap mass spectrometry, Heavy Ion Discussions, May 29th 2020, Physics Division, Argonne National Laboratory, IL (online).

Contributed talks:

(1) R. Sandler, Penning trap mass spectrometry Q-value determinations for highly-forbidden β-decay, Meeting of the APS Division Nuclear Physics, October 27th 2017, Pittsburg, PA.
(2) R. Sandler, Penning trap mass spectrometry Q-value determinations for highly-forbidden β-decay, APS April Meeting, April 15th 2018, Columbus, OH.
(3) N.D. Gamage, Development of CHIP-TRAP: the Central Michigan University High Precision Penning Trap, APS DNP/JPS Meeting, October 27th 2018, Hilton Waikoloa Village, Big Island, HI.
(4) M. Redshaw, Penning trap mass spectrometry Q value determinations for investigating ultra-low Q value β-decays, APS DNP/JPS Meeting, October 25th 2018, Hilton Waikoloa Village, Big Island, HI.
(5) N.D. Gamage, Recent progress in the development of the CHIP-TRAP mass spectrometer, APS DNP Meeting, October 17th 2019, Crystal City, VA.
(6) N.D. Gamage, Precise Q value measurements of ^{112,113}Ag and ^{115}Cd with the Canadian Penning Trap for evaluation of potential ultra-low Q value β-decays, APS April 2021 (online).
(7) R. Bhandari, Design and Status of a Multi-Reflection Time-of-Flight Mass Separator for the CHIP-TRAP Penning Trap Mass Spectrometer at Central Michigan University, APS DNP Meeting October 12th 2021 (online).
(8) M. Horana Gamage, Design and Operation of a Penning Ion Trap Source for the CHIP-TRAP Mass Spectrometer, APS DNP Meeting October 12th 2021 (online).
(9) M. Horana Gamage, Design and Operation of a Penning Ion Trap Source for the CHIP-TRAP Mass Spectrometer, International Conference on Ion Sources (ICIS2021), September 20th 2021 (online).
(10) M. Horana Gamage, Precise mass measurement of ^{75}As for evaluation of ultra-low Q value β-decay branches in ^{75}Se and ^{75}Ge, APS April Meeting 2022, April 11th 2022, New York, NY.

Contributed Posters:

(1) N.D. Gamage, Status of CHIP-TRAP: The Central Michigan University High-Precision Penning trap, Advances in Radioactive Isotope Science (ARIS 2017), May 30th 2017, Keystone, CO.

(2) R. Sandler, Penning trap mass spectrometry Q-value determinations for highly-forbidden and low Q-value β-decay processes, Advances in Radioactive Isotope Science (ARIS 2017), May 30th 2017, Keystone, CO.
(3) J. Peck, Laser Ablation Source Operation and Characterization of Ion Sources, APS Conference for Undergraduate Women in Physics (CUWiP), January 12th – 14th 2018, Toledo, OH.
(4) R. Bhandari, Status of CHIP-TRAP: The Central Michigan University High-Precision Penning trap, APS April Meeting, April 16th 2018, Columbus, OH.
(5) M. Horana Gamage, Development of an electron impact ionization source for the CHIP-TRAP apparatus, APS April Meeting, April 16th 2018, Columbus, OH.
(6) N.D. Gamage, Penning Trap Mass Spectrometry Q Value Determinations for Investigating Ultra-low Q value β-decays, 7th International Conference on Trapped Charged Particles and Fundamental Physics, October 2nd 2018, Traverse City, MI.
(7) M. Horana Gamage, Status of CHIP-TRAP: the Central Michigan University High Precision Penning Trap, 7th International Conference on Trapped Charged Particles and Fundamental Physics, October 2nd 2018, Traverse City, MI.
(8) M. Redshaw, Precise Penning trap Q value measurements for nuclear and neutrino physics, Nuclear Chemistry Gordon Conference, June 16th – 21st 2019, New London, NH.
(9) P. Snoad, Design and construction of an MR-TOF-MS for the CHIP-TRAP Penning trap mass spectrometer at Central Michigan University, APS DNP Meeting, October 15th 2019, Crystal City, VA.
(10) R. Bhandari, Design and Status of a Multi-Reflection Time-of-Flight Mass Separator for the CHIP-TRAP Penning Trap Mass Spectrometer at Central Michigan University, APS April Meeting 2021 (online).
(11) R. Bhandari, Precise Measurement of the ^{7}Be and ^{163}Ho Electron Capture Q-value for Neutrino Studies, International Conference on Ion Sources (ICIS2021), September 20th 2021 (online).
(12) R. Bhandari, First direct measurement of the ^{7}Be electron capture Q value to aid experimental searches for sterile neutrinos with the BeEST, APS April Meeting 2022, April 11th 2022, New York, NY.

Table 4: Summary of publications since the beginning of the award on which individuals are an author. Individual is an author (individual played a leading or substantive role).

Name	Letter Publications	Other Refereed Journals	Invited Talks
Faculty/permanent staff			
M. Redshaw	2(0)	9(5)	6
Graduate Students			
N. Gamage		4(2)	
R.M.E.B Kandegedara		1(1)	
R. Sandler	2(0)	8(2)	
R. Bhandari		2(0)	
M. Horana Gamage		2(1)	
J. Dissanayaki		1(0)	
Total	**2(0)**	**9(5)**	**6**